Journal of Materials Chemistry A

ROYAL SOCIETY OF CHEMISTRY

PAPER

Cite this: J. Mater. Chem. A, 2021, 9, 24472

Modulating the thermal conductivity of crystalline nylon by tuning hydrogen bonds through structure poling†

Shichen Deng,[a] Dengke Ma,*[b] Guangzu Zhang [c] and Nuo Yang *[a]

Received 30th June 2021
Accepted 7th October 2021

DOI: 10.1039/d1ta05519d

rsc.li/materials-a

The low thermal conductivity of polymers affects the reliability and functionality of devices. Tuning the hydrogen bonds inside them is one strategy to modulate their thermal conductivity. Here, using molecular dynamics simulation, we show that the thermal conductivity of crystalline odd-numbered nylons can be modulated by tuning the hydrogen bonds inside them through structure poling. Thermal conductivities along all directions can be increased after poling, and the thermal conductivity along the polarization direction in nylon 5 increases by a factor of three. Further analysis of morphology, H-bonds and vDOS shows that the increased density of inter-chain hydrogen bonds provides more effective heat conduction paths, and enhances structural order to facilitate phonon transport. And the change ratio of thermal conductivity after poling decreases as the nylon number increases. Investigation of thermal conductivity *versus* the electric field shows that the enhancement is transient after the field exceeds the threshold. Our study provides useful insight into the regulation of thermal transport in polymers.

Introduction

Polymers have been applied in a wide variety of applications including structural materials, electronic packaging, soft robotics and artificial skin because they are lightweight, low-cost, durable and corrosion-resistant.[1–3] However, the low thermal conductivity (0.1–0.3 W m^{-1} K^{-1})[4,5] of polymers largely limits their applications in thermal management of microelectronics, sensors and energy storage which require high thermal conductivity to dissipate heat as efficiently as possible. If the thermal conductivity of polymers can be tuned to a high value, they can replace traditional heat conductors, such as metals[6] and ceramics,[7] which could promote the progress of various industries because of the many unique advantages of polymers. Thus, tuning the thermal conductivity of polymers is of tremendous scientific interest and practical application significance.

In polymers, intra-chain covalent bonding interactions and inter-chain non-bonding interactions both contribute to thermal transport.[8,9] The high κ simulated[10,11] and measured in aligned polymer chains[12,13] suggests that heat is transferred much more efficiently along the covalently bonded chains than between chains with non-bonding interactions. However, the inter-chain interactions can also influence both the inter-chain and intra-chain thermal transport by influencing the conformation of polymers.[14,15] For example, the thermal conductivity of poly(vinylsulfonic acid Ca salt)[16] could be as high as 0.67 W m^{-1} K^{-1} due to the relatively strong electrostatic forces between the ions in different polymer chains. And it is reported that the vdW confinement can result in more than two-fold enhancement in the thermal conductivity of both polyethylene single-chains,[17] because the confined vdW potential barriers reduce the atomic thermal displacement magnitudes, leading to less phonon scattering.

The hydrogen bond (H-bond) is another inter-chain interaction and it is 10–100 times stronger than the vdW interaction.[18] H-bonds in polymers can enhance existing thermal pathways or create new ones to more efficiently conduct heat.[19] Therefore, increasing the concentration of H-bonds could lead to higher thermal conductivity. For example, it is reported that the thermal conductivity of a blend of poly(*N*-acryloyl piperidine) and poly(acrylic acid)[20] can reach over 1.5 W m^{-1} K^{-1} because H-bonds inside it contribute to form a dense and homogeneously distributed thermal network. And Xie *et al.*[21] found that polymers with the ability to form H-bonds are more thermally conductive than typical glassy polymers due to the stronger intermolecular interactions when studying the thermal conductivity of spin-coated water-soluble polymers.

In previous studies[20,22] that utilize H-bonds to modulate the thermal conductivity of polymers, H-bonds are usually controlled

[a]State Key Laboratory of Coal Combustion, School of Energy and Power Engineering, Huazhong University of Science and Technology (HUST), Wuhan 430074, P. R. China. E-mail: nuo@hust.edu.cn

[b]NNU-SULI Thermal Energy Research Center (NSTER), Center for Quantum Transport and Thermal Energy Science (CQTES), School of Physics and Technology, Nanjing Normal University, Nanjing, 210023, P. R. China. E-mail: dengke@njnu.edu.cn

[c]School of Optical and Electronic Information, Wuhan National Laboratory of Optoelectronics, Huazhong University of Science and Technology (HUST), Wuhan, 430074, P. R. China

† Electronic supplementary information (ESI) available. See DOI: 10.1039/d1ta05519d

by chemical approaches in the synthetic process. However, after the sample is successfully synthesized, it is unlikely to modulate its thermal conductivity once more. Is there any method that can change the H-bonds and thus modulate the thermal conductivity after the material is synthesized? Attention is turned to odd-numbered nylon, which is a kind of hydrogen-bonded polymer,[23] and also a kind of ferroelectric polymer.[24] It is shown that the structure of odd-numbered nylon has unpoled and poled situations.[25,26] In addition, previous studies have shown that the electric field can modulate the thermal conductivity of other ferroelectric materials like $BiTiO_3$ (ref. 27) and poly(vinylidene fluoride)[28] by poling their structures. Therefore, could the thermal conductivity of odd-numbered nylons be modulated by changing the H-bonds inside them through structure poling? It is interesting and worth investigating.

In this work, the structure poling effect on the thermal conductivities of crystalline odd-numbered nylons is numerically investigated. Firstly, four kinds of odd-numbered nylons arrays (nylon 5, nylon 7, nylon 9 and nylon 11) are constructed. Then, thermal conductivities of these unpoled and poled nylons are investigated and compared. Then, the mechanism of structure poling effect on thermal transport is discussed by studying changes in the structure morphology, H-bonds and phonon properties. Lastly, different electric fields are applied to unpoled nylon 5 to see the thermal conductivity change.

Structure and method

The structures of nylon structures are shown in Fig. 1. Fig. 1(a) gives the monomer of nylon 5, nylon 7, nylon 9 and nylon 11. Nylon consists of numerous copies of [–NH–CO–$(CH_2)_{n-1}$–], where n denotes the number of carbon atoms in each repeat unit. In odd-numbered nylon, the n is odd, and different numbers of n lead to different nylon materials. For example, nylon 5 has the molecular structure [–NH–CO–$(CH_2)_4$–]. Each monomer contains an amide group, which possesses strong polarity. And in a single chain, all amide groups orient towards the same direction, so the single nylon chain is always poled. Fig. 1(b) and (c) show the structure of unpoled and poled nylon arrays which are constructed by aligning 36 straight nylon chains in a triclinic lattice, with periodic boundary conditions applied in all three spatial directions. In unpoled structures, half of the chains orientate oppositely with the other half of the chains along the y-direction (direction of single-chain polarity). Although every single chain possesses a polarity, their polarities cancel each other out, resulting in a nonpolar property of the unpoled system. In contrast, in the poled system, all the chains are oriented in the same direction, so their polarities can be added, which results in a polar property of the whole system. For ease of expression, abbreviations are used as UN-n (unpoled nylon) and PN-n (poled nylon). For example, UN-5 represents unpoled nylon 5, and PN-5 represents poled nylon 5.

The equilibrium molecular dynamics (EMD) simulation method is used to calculate the thermal transport properties.[29–31] All EMD simulations in this work are performed using the large-scale atomic/molecular massively parallel simulator (LAMMPS) package.[32–34] The interactions between atoms are described by the polymer consistent force field (PCFF),[35] which includes anharmonic bonding terms and is intended for applications in polymers and organic materials. And the PCFF parameters are directly adopted from BIOVIA Materials Studio.[36] Scheme S1† lists the partial charges and LJ (12–6)

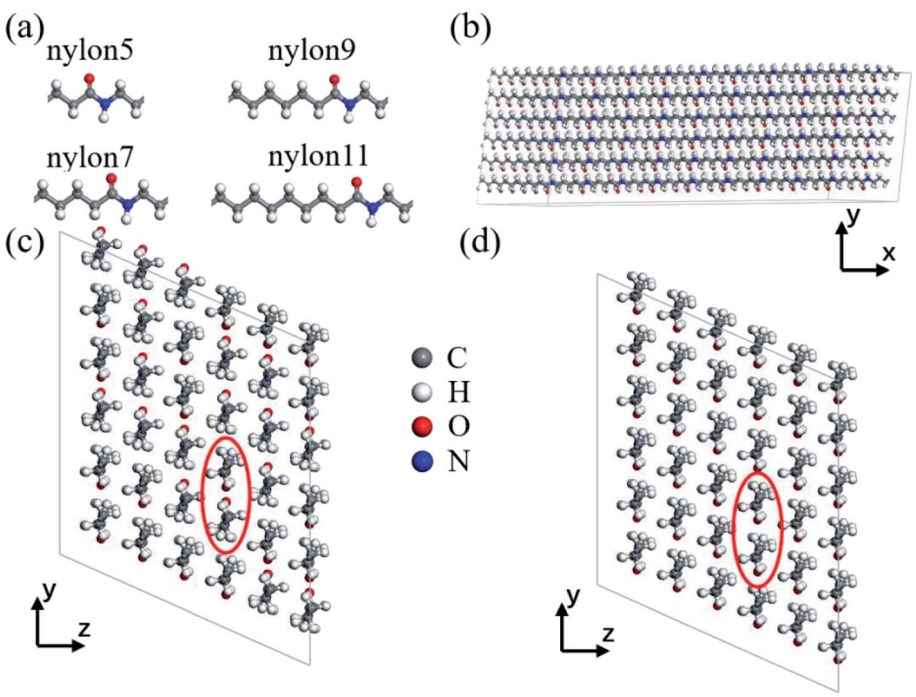

Fig. 1 (a) Single-chain structure of different numbered nylons; (b) array of nylon chain; inter-chain structure of (c) unpoled and (d) poled nylon arrays.

potential parameters of all atom types. The long-range coulombic force is calculated using the standard Ewald summation with an error parameter of 10^{-4}.[37] The velocity Verlet algorithm is employed to integrate equations of motion.[38] 0.25 fs and 10 Å are chosen as the time step and cutoff distance for the Lennard–Jones interaction, respectively. The structures are primarily simulated in NPT ensembles at 300 K temperatures and 1 atm for 100 ps to obtain the optimized structures and simulation cell sizes, followed by NVE ensembles for 100 ps before collecting heat flux of all three directions (along-chain direction x, and inter-chain directions y and z) in NVE ensembles for 4 ns. In addition, five independent simulations with different initial conditions are conducted by assigning different initial velocities to atoms in the system to get a better average (more MD simulation details are given in S1†).

Results and discussion

The thermal conductivity results of unpoled and poled structures of different odd-numbered nylons along x (along-chain), y (inter-chain direction parallel to the polarization direction) and z (inter-chain direction perpendicular to the polarization direction) directions at 300 K are shown in Fig. 2. Before studying the thermal conductivity, the convergence of thermal conductivity with respect to the simulation cell size was confirmed as shown in Fig. S1.† The heat current flow autocorrelation function (HCACF) and its integral along all directions at 300 K are shown in Fig. S2 and S3,† respectively. In UN-5, κ_x, κ_y, and κ_z are 6.58 ± 0.58, 0.30 ± 0.05 and 0.25 ± 0.01 W m^{-1} K^{-1}, respectively. The along-chain κ_x is much higher than the inter-chain κ_y and κ_z. The anisotropic thermal transport is due to the strong covalent bonds along the chain but weak non-bonded interactions along the inter-chain directions. After poling, thermal conductivities along all three directions are improved. In PN-5, κ_x, κ_y, and κ_z are 11.49 ± 0.16, 0.90 ± 0.08 and 0.37 ± 0.04 W m^{-1} K^{-1}. The increase ratios of κ_x, κ_y, and κ_z are 75%, 200%, 48%, respectively. The magnitude of value change along the polarization direction is larger than that in poly(vinylidene fluoride) which is from 0.16–0.50 W m^{-1} K^{-1}.[28]

As the nylon number increases, the change range of thermal conductivity decreases. In UN-11, κ_x, κ_y, and κ_z increase to 9.45 ± 0.78, 0.26 ± 0.03 and 0.33 ± 0.01 W m^{-1} K^{-1}, respectively. In PN-11, these values increase to 13.50 ± 0.81, 0.52 ± 0.05 and 0.41 ± 0.03 W m^{-1} K^{-1}, respectively. The increase ratios are 43%, 100%, 24%, respectively. In addition, as the nylon number increases, κ_x of both unpoled and poled nylon increases. In unpoled nylons, κ_y is slightly reduced when the nylon number increases from 5 to 7, and then remains almost unchanged as the nylon number continues to increase. However, κ_y of poled nylon decreases significantly with the increase of the nylon number, while κ_z shows a slightly upward tendency in both unpoled and poled structures.

To study the origin of thermal conductivity change, the relaxed structures are first investigated. The structure plots in the xz plane of all simulated structures shown in Fig. S4† indicate that all molecular chains are still arranged in a form of an array. This is because the periodic boundary condition is applied to all directions in our simulation, the length of molecular chains is infinite and not easy to curl, and the chain at the box boundary will have a ghost chain out of the box interacting with it and make it balanced by force. Thus, the array structure can be well maintained below its melting point which is much higher than 300 K.[39] And this phenomenon is also common in other crystalline polymers such as crystalline PE and PEO.[31,40] The strong covalent bonds dominate the along-chain heat transport, generating high κ_x of unpoled and poled nylons.

However, the discrepancy in inter-chain morphology between unpoled and poled nylons is significant. As can be seen in Fig. 3(a), for UN-5, the inter-chain orientations of molecular chains are inconsistent. Take the positions of oxygen atoms for example, the oxygen atoms in some chains are at the top of the

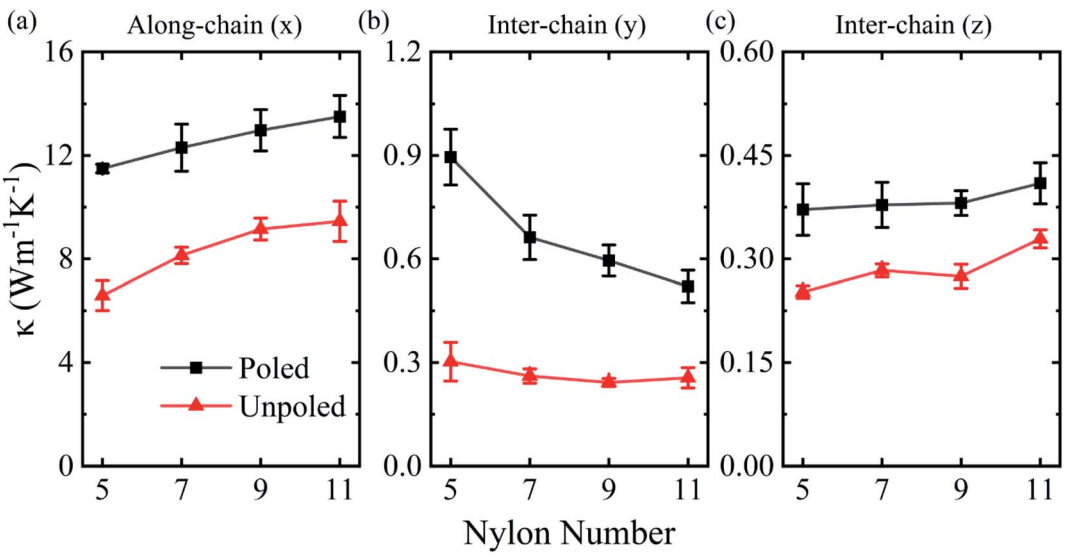

Fig. 2 Thermal conductivity of different poled and unpoled odd-numbered nylons along (a) x, (b) y and (c) z directions at 300 K.

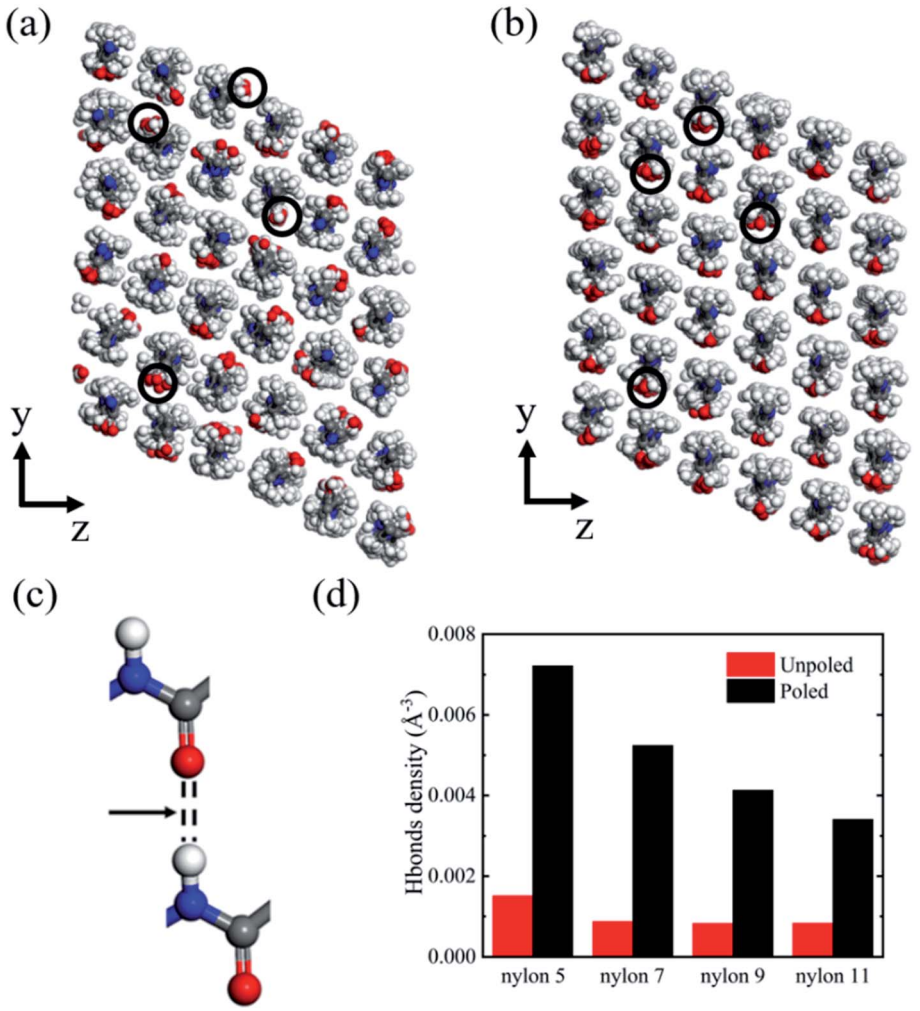

Fig. 3 Structure plots in the *yz* plane after relaxation of (a) UN-5; (b) PN-5. The black circle denotes the positions of oxygen atoms in some molecular chains. In UN-5, the oxygen atoms lie at the top in some chains but lie at the bottom in other chains. In PN-5, the oxygen atoms all lie at the bottom of the chains. (c) Schematic of H-bonds in nylon; (d) the density of H-bonds in different structures.

chain, but in other chains, the oxygen atoms are at the bottom of the chains, as denoted by small black circles. Each molecular chain rotates at different angles around its carbon skeleton, making it difficult to form H-bonds between molecular chains. In contrast, in the relaxed structure of PN-5, as shown in Fig. 3(b), the orientations of all molecular chains along *y* and *z* directions are highly consistent, and the oxygen atoms all lie at the bottom of the chains, which gives a high probability to form H-bonds between molecular chains. Similar morphological differences can also be observed in unpoled and nylon 7, nylon 9 and nylon 11 (see Fig. S5†).

Then, the number changes of H-bonds after structure poling are counted. H-bonds can provide more paths for thermal transport, and they are much stronger than the vdW interaction, which enables them to conduct heat more efficiently.[41] The diagram of the H-bond is shown in Fig. 3(c), which show that a hydrogen atom in an amide group of one chain formed an H-bond with an oxygen atom in an amide group of a neighboring chain. The formation of hydrogen bonds needs to meet the distance and angle conditions between atoms which are illustrated in detail in S6,† so it is possible that the hydrogen bonds form along the polarization direction (*y*-direction in this work). The average densities of hydrogen bonds in unpoled and poled structures of different nylons over 20 ps run are calculated (see Fig. S6†), as shown in Fig. 3(d). It is clearly seen that after poling, densities of H-bonds in all four odd-numbered nylons show a dramatic increase, which could explain the largest change ratio of κ_y after poling, as well as the much higher κ_y than κ_z in poled nylons. And for poled nylons, the density of H-bonds decreases with increasing nylon numbers, which leads to a decreased κ_y. The large density of H-bonds in PN-5 results in a larger change magnitude of thermal conductivity in nylon 5 than that in PVDF.[28] Moreover, among unpoled nylons, the density of H-bonds in UN-5 is slightly higher while the others are almost the same, which could explain the slightly larger κ_y of UN-5 and the similar κ_y of other unpoled nylons.

However, κ_x and κ_z show different dependence on the nylon number with κ_y: κ_x shows a clear upward trend, and κ_z shows

a slightly upward trend as the nylon number increases. The along-thermal conductivities of nylons are lower than that of polyethylene due to both the bond-strength disorder and mass disorder in the chain compared to polyethylene.[42] The amide groups incorporated into the aliphatic pristine chains can be viewed as a mass disorder, and the C–N bonds along the backbone can be viewed as a bond-strength disorder. Generally, these disorders in the chain create localized vibrational modes, which impede the energy transport by delocalized, long-wavelength phonon modes and significantly reduce the thermal conductivity as that in alloys.[43] And as the nylon number increases, the density of the amide group decreases, and the suppression of the thermal conductivity becomes weaker, which could explain the larger κ_x of larger-number nylon. And this tendency is consistent with other's MD results about thermal conductivities of different single even-numbered nylon chains.[44] Similarly, along the z-direction, where no hydrogen bonding interaction exists, the amide groups act as a phonon scatterer and suppress κ_z. And κ_z shows a slightly upward tendency with increasing nylon number because of the decreased density of amide groups.

To further study the influence of H-bonds on the morphology of odd-numbered nylons, radial distribution function (RDF) of carbon atoms and distribution of the dihedral angles are calculated for unpoled and poled nylons (details of calculating RDF are given in S7†). The inter-chain and along-chain RDF results of UN-5 and PN-5 at 300 K are shown in Fig. 4(a) and (b), respectively. In PN-5, the peaks of inter-chain RDF become sharper compared with those in UN-5, indicating a limited inter-chain motion range and stronger constraining forces because of the increase of H-bonds, which would suppress anharmonic phonon scattering and lead to an enhanced inter-chain thermal conductivity. The peaks of inter-chain RDF in PN-5 are also sharper than those in UN-5, indicating the restricted motion of atoms along the chain backbone. Moreover, in the distribution of the dihedral angles in UN-5 and PN-5, as shown in Fig. 4(c), there are sharper peaks in PN-5 than those in UN-5, which means that there are weaker torsional motions of chains in PN-5 than that in UN-5 because of the constraint of H-bonds. The above results suggest that the arrangement of chains in PN-5 is more ordered because of the increased H-bonds, which leads to higher thermal conductivities in both inter-chain and along-chain directions. Similar changes in RDF and distributions of the dihedral angles after poling are also observed in nylon 7, nylon 9 and nylon 11 (see Fig. S7–S9,† respectively).

To gain further understanding of the structure poling effect on thermal conductivity, the vibrational density of states (vDOS) is calculated to qualitatively analyze the difference in heat conduction among unpoled and poled odd-numbered nylon structures. The results of vDOS in the full-frequency range are given in Fig. S10.† Keeping in view that dominant thermal energy carriers in crystalline polymers are usually low-frequency phonons,[8] enlarged curves of vDOS of unpoled and poled nylons in the frequency range below 20 THz are presented in Fig. 5. As can be seen, in all directions in Fig. 5(a), some peaks in vDOS of UN-5 are wider and flatter, or even indistinct compared with that in PN-5, which means that some phonon modes near the

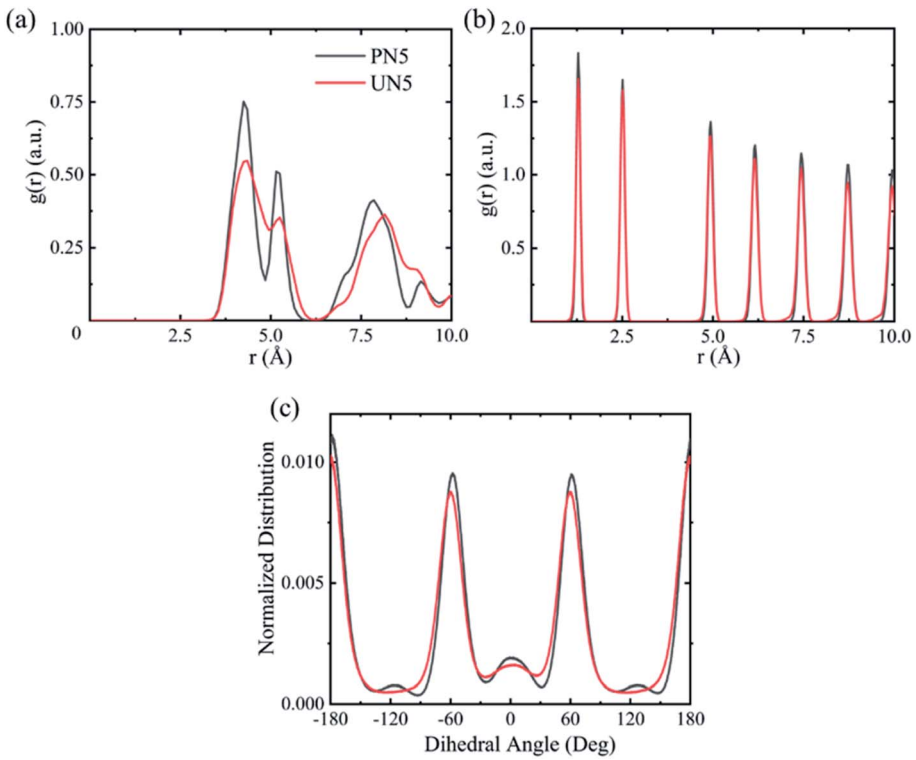

Fig. 4 (a) Inter-chain radial distribution function; (b) along-chain radial distribution function; (c) distribution of dihedrals of UN-5 and PN-5.

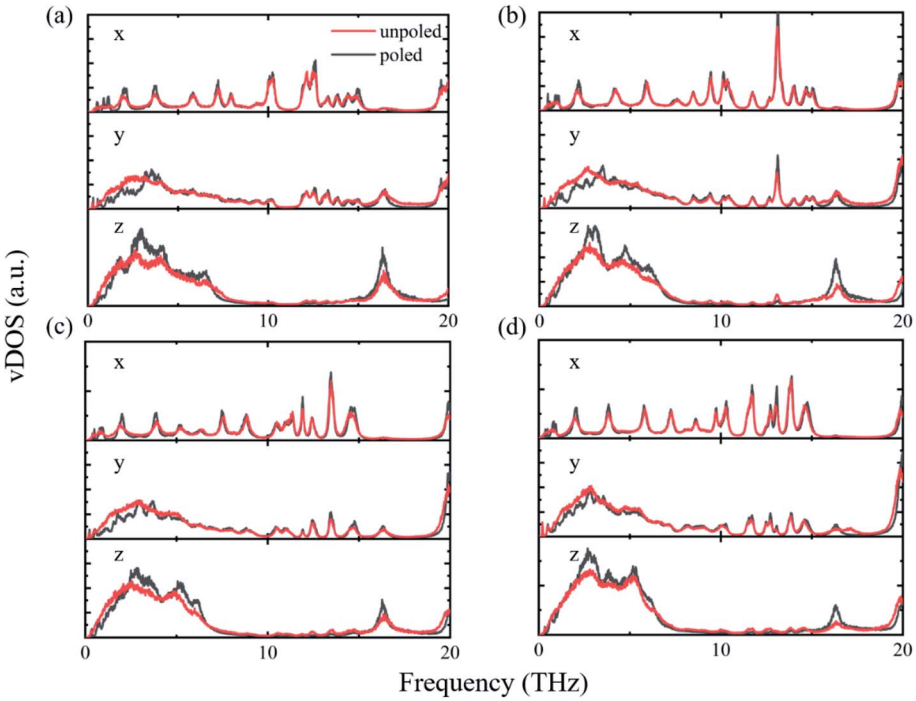

Fig. 5 vDOS comparation between unpoled and poled structures of (a) nylon 5; (b) nylon 7; (c) nylon 9 and (d) nylon 11 below 20 THz.

frequencies of peaks scatter to other frequencies.[8] The severe anharmonic phonon scattering results in low thermal conductivity of UN-5. And the sharper peaks in vDOS of PN-5 indicate that the anharmonic phonon scattering is suppressed, resulting in higher thermal conductivity of PN-5.

Furthermore, along the *y*-direction, a blue shift of vibrational modes below 2 THz in PN-5 can be observed compared with that in UN-5. From the formula based on the Debye hypothesis which could be used to roughly estimate the DOS ($g(\omega)$) of low-frequency modes:

$$g(\omega) = 3V\omega^2/(2\pi C^3) \quad (1)$$

where V is the volume, ω is the frequency, and C is the group velocity, respectively. It can be concluded that a smaller DOS at the same frequency corresponds to a higher group velocity. Thus, the blue shift of DOS in PN-5 means higher phonon group velocities of the low-frequency vibrational modes in PN-5. The increase of H-bonds along the *y*-direction could increase the elasticity modulus[45] of nylons in this direction because of the stronger bonding strength of H-bonds than that of van der Waals force, which makes the material harder along this direction. And the hardening effect can increase the frequencies of phonons and their group velocities.[46,47] Thus, the higher κ_y of PN-5 is attributed to suppressed phonon scattering and higher phonon group velocities. And in nylon 7, nylon 9 and nylon 11, there are similar discrepancies between unpoled and poled structures, as shown in Fig. 5(b), (c) and (d), respectively. However, these discrepancies become smaller in larger-number nylon, which could explain the downward tendency of the thermal conductivity change ratio as the nylon number increases.

The poled nylon structures we simulated above are artificially constructed, not obtained by poling the unpoled nylon structures with an electric field, which is a very ideal situation and could provide theoretical guidance. To see whether the electric field can induce structure poling in unpoled nylons, UN-5 is simulated under different electric fields as an example. The system is first simulated in NPT ensembles at 300 K and 1 atm for 100 ps, followed by NVE ensembles for 100 ps. Then the electric field is applied to UN-5 along the *y*-direction, also simulated in NPT ensembles at 300 K and 1 atm for 100 ps followed by NVE ensembles for 100 ps. Afterward, the electric field is removed, followed by the same steps that are used to calculate thermal conductivities.

The calculated κ_x, κ_y and κ_z after relaxing at different electric fields are shown in Fig. 6. When the electric field intensity is below 2 V nm^{-1}, inter-chain thermal conductivities are almost the same as that of the initial unpoled structure, and hardly change with the electric field. However, the inter-chain thermal conductivities suddenly increase to the value approaching that of PN-5 when the electric field intensity exceeds 2 V nm^{-1}. This thermal conductivity switch behavior is very similar to the polarization switching phenomenon in ferroelectric polymers.[48,49] And the threshold electric field between 1.5 and 2 V nm^{-1} is close to the value of other numerical simulations[50,51] of ferroelectric materials.

To explain the switch behavior of thermal conductivity, the relaxed structures of UN-5 under different electric fields are compared, as shown in Fig. S11.† It is clear that the structure relaxed below 2 V nm^{-1} has a poor inter-chain arrangement. The red oxygen atoms in some chains are located in the upper half of the chains, but in other chains, the oxygen atoms are

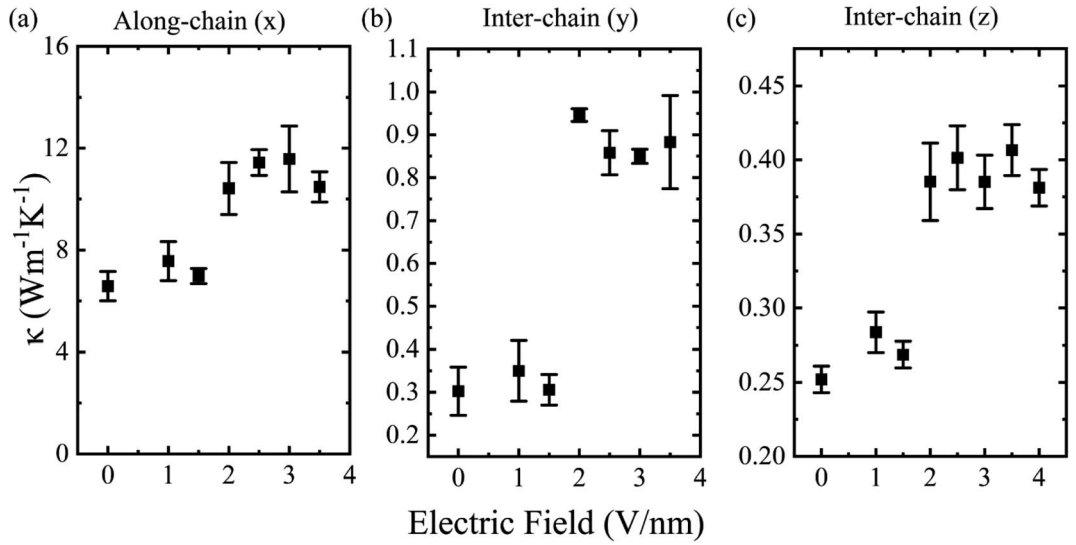

Fig. 6 The thermal conductivities of UN-5 *versus* the electric field intensity along three directions: (a) along-chain, *x*; (b) inter-chain, *y*; (c) inter-chain, *z*. The structure was relaxed in electric fields of different values of intensity.

located in the lower half of the chains, which means that the orientations of these chains are random. In contrast, when applying an electric field over 2 V nm^{-1}, molecular chains in UN-5 reorient to the same direction (the red oxygen atoms are all located in the lower half of the chains), which means a higher inter-chain lattice order and leads to an increase in thermal conductivity. The attached animation clearly shows the structure change process of UN-5 under a 3 V nm^{-1} electric field. In this animation, all molecular chains gradually rotate in the same direction and then vibrate near their equilibrium positions. And over 2 V nm^{-1}, the morphology would not have a noticeable change, so the thermal conductivity shows no obvious change over the threshold electric field. Therefore, this thermal conductivity switch behavior mainly originates from morphological mutation induced by the electric field.

Conclusion

In summary, we have performed MD simulations to investigate the structure poling effect on the thermal transport in crystalline odd-numbered nylons. In the poled structures, thermal conductivities in crystalline nylon 5, nylon 7, nylon 9 and nylon 11 along all three directions at 300 K are enhanced compared with that of unpoled structures. The thermal conductivity enhancement ratio along the polarization direction is the most significant, especially in nylon 5, from 0.30 to 0.90 W m^{-1} K^{-1}. As the nylon number increases, the change range of thermal conductivity decreases. The RDF and dihedral distribution results show that the stronger inter-chain and along-chain order contribute to the enhanced thermal conductivity of the poled structure. The H-bonds analysis reveals that the increased density of H-bonds leads to a dramatic increase of thermal conductivity along the polarization direction. Then, the vDOS results show that the morphology changes and increase of H-bonds lead to suppressed phonon scattering and higher phonon group velocities in the poled structure. In addition, as the nylon number increases, the changes in H-bonds and vDOS after poling become smaller, which explains the decreased change ratio of thermal conductivity in large-number nylon. Moreover, thermal conductivities of UN-5 simulated in different electric fields are calculated, and the results show that thermal conductivity could be enhanced only if the electric field exceeds the threshold. Structure poling by applying an external electric field has advantages including *in situ* flexibility, quick response and low power consumption.[52–54] This finding is promising to be applied in fields such as thermal management, flexible electronics and thermal switches.

Conflicts of interest

The authors declare no competing financial interests.

Acknowledgements

This work is financially supported by the National Key Research and Development Project of China (2018YFE0127800), Fundamental Research Funds for the Central Universities (2019kfyRCPY045) and Program for HUST Academic Frontier Youth Team. The authors thank the National Supercomputing Center in Tianjin (NSCC-TJ) and China Scientific Computing Grid (ScGrid) for providing assistance in computations.

References

1 Z. L. Wang, *Adv. Mater.*, 2012, **24**, 280–285.
2 X. Chen, Y. Su, D. Reay, *et al.*, *Renewable Sustainable Energy Rev.*, 2016, **60**, 1367–1386.
3 Y. Cai, L. Huo and Y. Sun, *Adv. Mater.*, 2017, **29**, 1605437.
4 H. Y. Chen, V. V. Ginzburg, J. Yang, *et al.*, *Prog. Polym. Sci.*, 2016, **59**, 41–85.

5 X. Xu, J. Chen, J. Zhou, *et al.*, *Adv. Mater.*, 2018, **30**, 1705544.
6 M. Peplow, *Nature*, 2016, **536**, 266.
7 S. Deng, C. Xiao, J. Yuan, *et al.*, *Appl. Phys. Lett.*, 2019, **115**, 101603.
8 X. Yu, R. Li, T. Shiga, *et al.*, *J. Phys. Chem. C*, 2019, **123**, 26735–26741.
9 X. Xu, J. Zhou and J. Chen, *Adv. Funct. Mater.*, 2019, **30**, 1904704.
10 A. Henry and G. Chen, *Phys. Rev. Lett.*, 2008, **101**, 235502.
11 Z. Zhang, Y. Ouyang, Y. Guo, *et al.*, *Phys. Rev. B*, 2020, **102**, 195302.
12 X. Huang, G. Liu and X. Wang, *Adv. Mater.*, 2012, **24**, 1482–1486.
13 S. Shen, A. Henry, J. Tong, *et al.*, *Nat. Nanotechnol.*, 2010, **5**, 251–255.
14 X. Wei, T. Zhang and T. Luo, *Phys. Chem. Chem. Phys.*, 2016, **18**, 32146–32154.
15 Y. Ouyang, Z. Zhang, Q. Xi, *et al.*, *RSC Adv.*, 2019, **9**, 33549–33557.
16 X. Xie, K. Yang, D. Li, *et al.*, *Phys. Rev. B*, 2017, **95**, 035406.
17 X. Yu, D. Ma, C. Deng, *et al.*, *Chin. Phys. Lett.*, 2021, **38**, 014401.
18 S. Thomas, *Angew. Chem., Int. Ed.*, 2002, **41**, 48–76.
19 C. Huang, X. Qian and R. Yang, *Mater. Sci. Eng., R*, 2018, **132**, 1–22.
20 G.-H. Kim, D. Lee, A. Shanker, *et al.*, *Nat. Mater.*, 2015, **14**, 295.
21 X. Xie, D. Li, T.-H. Tsai, *et al.*, *Macromolecules*, 2016, **49**, 972–978.
22 L. Mu, J. He and Y. Li, *J. Phys. Chem. C*, 2017, **121**, 14204–14212.
23 Y. He, B. Zhu and Y. Inoue, *Prog. Polym. Sci.*, 2004, **29**, 1021–1051.
24 B. Z. Mei, J. I. Scheinbeim and B. A. Newman, *Ferroelectrics*, 1993, **144**, 51–60.
25 V. Gelfandbein and D. Katz, *Ferroelectrics*, 2011, **33**, 111–117.
26 Y. S. Choi, S. K. Kim, M. Smith, *et al.*, *Sci. Adv.*, 2020, **6**, eaay5065.
27 C. Liu, V. Mishra, Y. Chen, *et al.*, *Adv. Theory Simul.*, 2018, **1**, 1800098.
28 S. Deng, J. Yuan, Y. Lin, *et al.*, *Nano Energy*, 2021, **82**, 105749.
29 A. J. H. McGaughey and M. Kaviany, *Adv. Heat Transfer*, 2006, **39**, 169–255.
30 M. An, B. Demir, X. Wan, *et al.*, *Adv. Theory Simul.*, 2019, **2**, 1800153.
31 H. Meng, X. Yu, H. Feng, *et al.*, *Int. J. Heat Mass Transfer*, 2019, **137**, 1241–1246.
32 S. Plimpton, *J. Comput. Phys.*, 1995, **117**, 1–19.
33 X. Wan, D. Ma, D. Pan, *et al.*, *Mater. Today Phys.*, 2021, **20**, 100445.
34 H. Meng, S. Maruyama, R. Xiang, *et al.*, *Int. J. Heat Mass Transfer*, 2021, **180**, 121773.
35 H. Sun, S. J. Mumby, J. R. Maple, *et al.*, *J. Am. Chem. Soc.*, 1994, **116**, 2978–2987.
36 BIOVIA, Dassault Systèmes, *BIOVIA Materials Studio, Version 8.0*, Dassault Systèmes, San Diego, 2014.
37 J. Kolafa and J. W. Perram, *Mol. Simul.*, 1992, **9**, 351–368.
38 W. C. Swope, H. C. Andersen, P. H. Berens, *et al.*, *J. Chem. Phys.*, 1982, **76**, 637–649.
39 N. Tsutsumi, N. Kajimoto, K. Kinashi, *et al.*, *J. Appl. Polym. Sci.*, 2019, **136**, 47595.
40 T. Zhang and T. Luo, *J. Appl. Phys.*, 2012, **112**, 094304.
41 G. Kikugawa, T. G. Desai, P. Keblinski, *et al.*, *J. Appl. Phys.*, 2013, **114**, 034302.
42 J. Liu and R. Yang, *Phys. Rev. B: Condens. Matter Mater. Phys.*, 2012, **86**, 104307.
43 S. Lepri, *Phys. Rep.*, 2003, **377**, 1–80.
44 L. Zhang, M. Ruesch, X. Zhang, *et al.*, *RSC Adv.*, 2015, **5**, 87981–87986.
45 H. Qiao, P. Qi, X. Zhang, *et al.*, *ACS Appl. Mater. Interfaces*, 2019, **11**, 7755–7763.
46 M. D. Gerboth and D. G. Walker, *J. Appl. Phys.*, 2020, **127**, 204302.
47 X. Meng, T. Pandey, J. Jeong, *et al.*, *Phys. Rev. Lett.*, 2019, **122**, 155901.
48 Q. M. Zhang, V. Bharti and X. Zhao, *Science*, 1998, **280**, 2101–2104.
49 G. Zhang, Q. Li, H. Gu, *et al.*, *Adv. Mater.*, 2015, **27**, 1450–1454.
50 V. S. Bystrov, *Phys. B*, 2014, **432**, 21–25.
51 V. S. Bystrov, N. K. Bystrova, E. V. Paramonova, *et al.*, *J. Phys.: Condens. Matter*, 2007, **19**, 456210.
52 X. Zheng, Z. Guo, D. Tian, *et al.*, *Adv. Mater. Interfaces*, 2016, **3**, 1600461.
53 Y. Liu, T. Zhou, Y. Zheng, *et al.*, *ACS Nano*, 2017, **11**, 8519–8526.
54 P. J. Hsu, A. Kubetzka, A. Finco, *et al.*, *Nat. Nanotechnol.*, 2017, **12**, 123–126.